

Efficient and bright green InP quantum dots light-emitting diodes enabled by a self-assembled dipole interface monolayer

Lufa Li,^a Yaning Luo,^a Qianqian Wu,^a Lin Wang,^a Guohua Jia,^b Tao Chen,^c Chengxi Zhang,^{*a} Xuyong Yang^{*a}

^aKey Laboratory of Advanced Display and System Applications of Ministry of Education, Shanghai University, 149 Yanchang Road, Shanghai 200072, China.

Email: Andrew_xiwa@shu.edu.cn; yangxy@shu.edu.cn

^bSchool of Molecular and Life Sciences, Curtin University, Perth, WA 6102, Australia.

^cOffice of Admissions and Career Services, Shanghai University, 99 Shangda Road, Shanghai 200444, China.

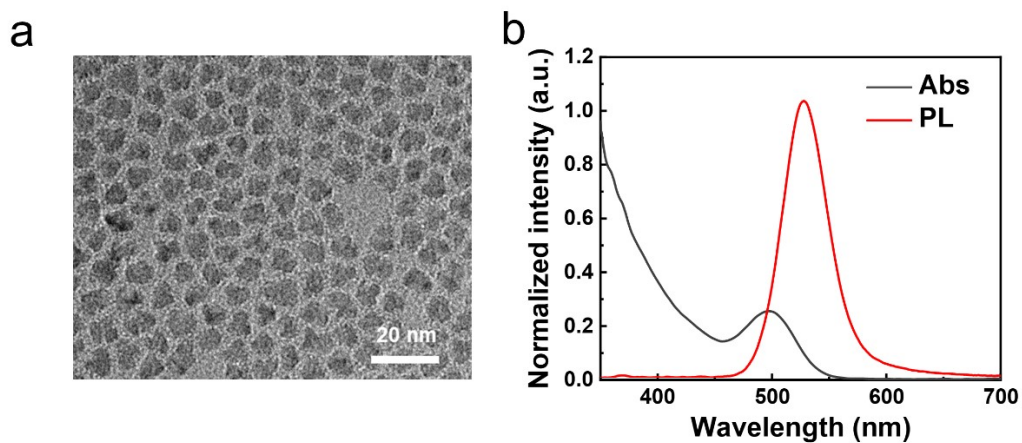


Figure S1 (a) TEM image and (b) PL & absorption spectra of green InP QDs.

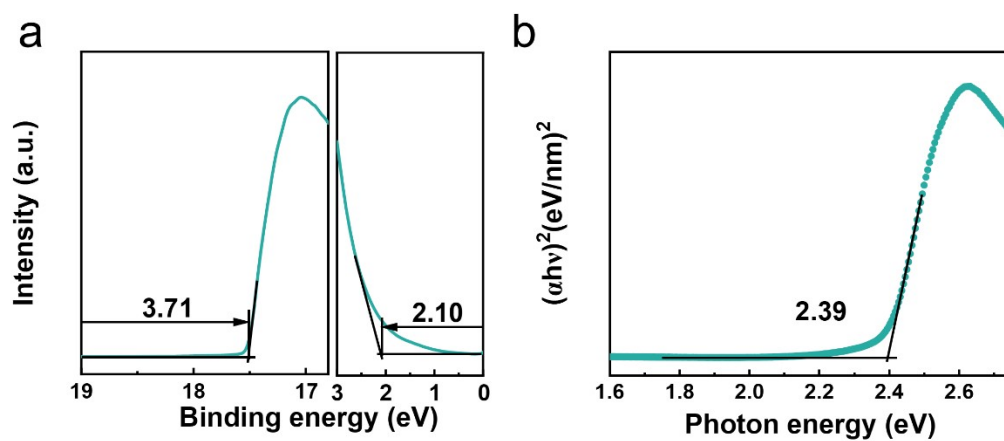


Figure S2 (a) UPS spectra of the secondary-electron cut-off region and the valence band edge region of InP QDs film. (b) Dependence of $(\alpha hv)^2$ of InP QDs film upon the incident photon energy (hv).

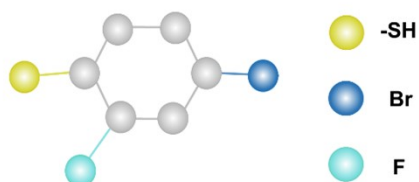


Figure S3 The BFTP molecular model.

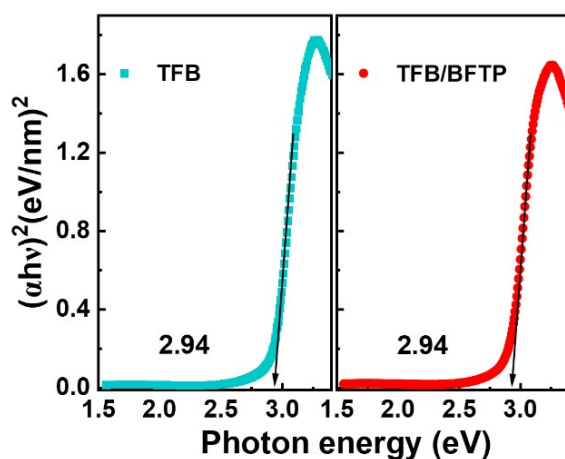


Figure S4 Dependence of $(\alpha h\nu)^2$ of TFB and TFB/BFTP films upon the incident photon energy ($h\nu$).

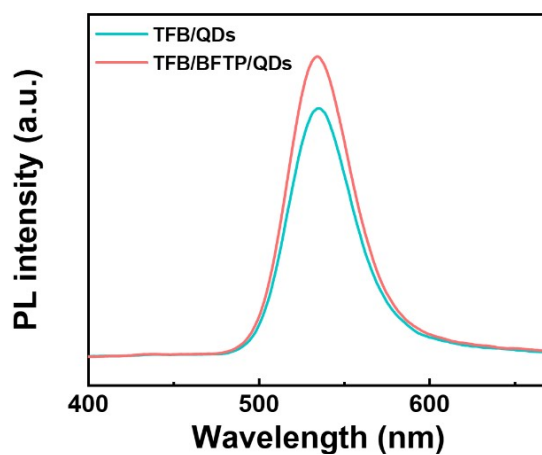


Figure S5 The PL intensity of InP QDs on TFB and TFB/BFTP films.

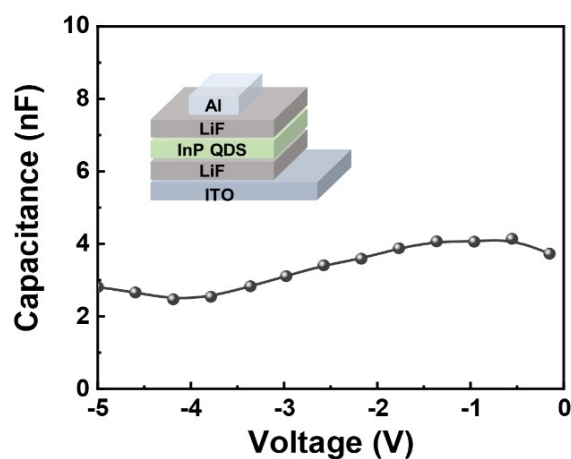


Figure S6 Relative dielectric constant (ϵ_r) extraction by the capacitance (C)-voltage (V) measurement.

The C - V curve was measured from the devices with the structure of ITO/LiF (40 nm)/perovskite/LiF(40 nm)/Al. By confirming the C value of HTL/InP QDs contact interface by the saturated part in the C - V curve towards negative voltage, we extracted the ϵ_r value of the contact interface by the following equation:

$$C = \frac{\epsilon_0 \epsilon_r S}{d}$$

where ϵ_0 , S and d represent vacuum permittivity, device area and thickness of the QDs film, respectively. The ϵ_r value was estimated to be 12.17.

The trap state density (n_{traps}) was determined using the trap-filled limit voltage equation:

$$n_{traps} = \frac{2\epsilon_0 \epsilon_r V_{TFL}}{ed^2}$$

where V_{TFL} is the intersection voltage of the trap-filled limit and ohmic regime, and e is the elemental charge.

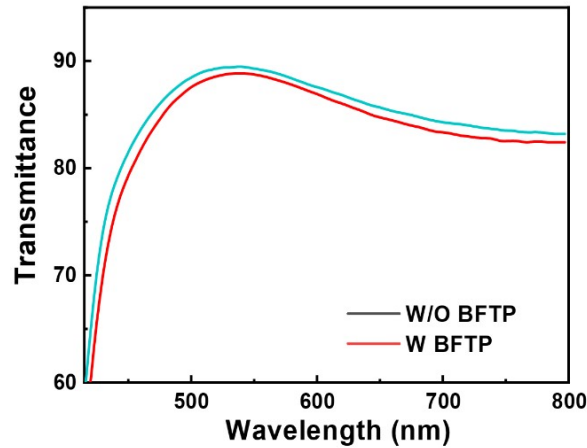


Figure S7 Transmittance spectra for TFB (W/O BFTP) and TFB/BFTP (W BFTP) films on ITO substrate.

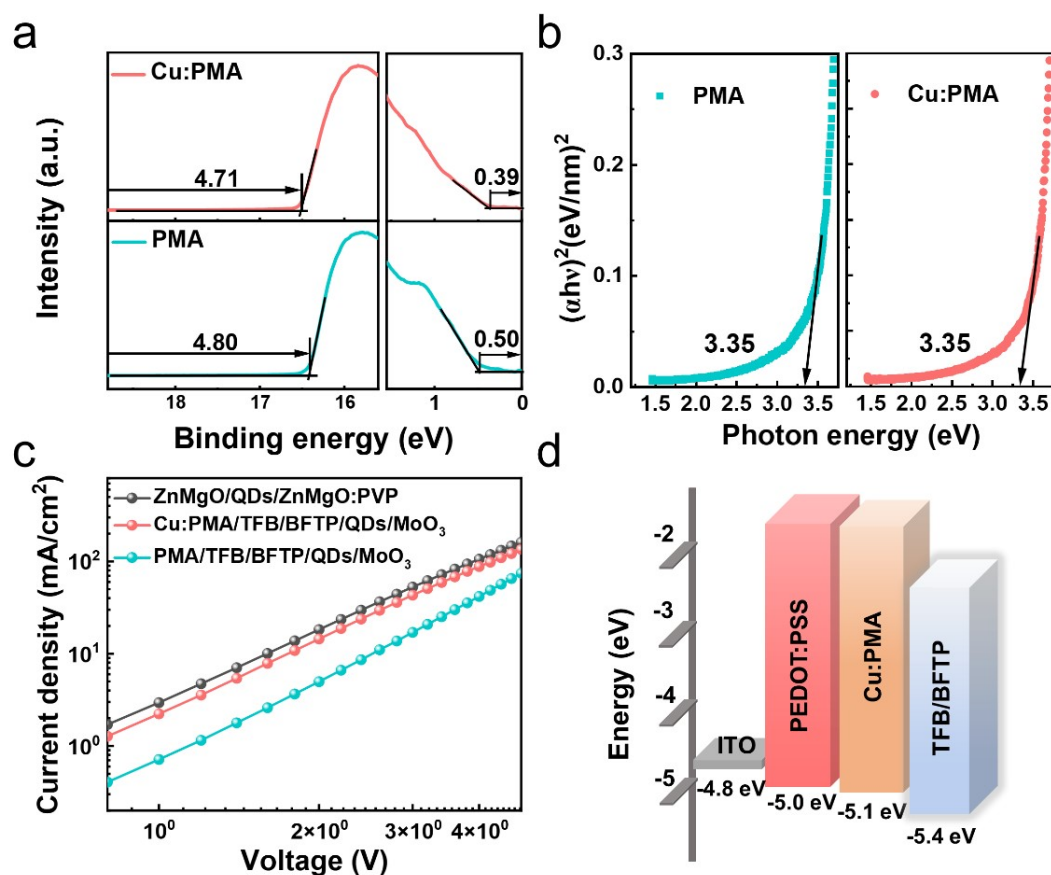


Figure S8 (a) UPS spectra of the secondary-electron cut-off region and the valence band edge region of PMA and Cu: PMA films deposited on ITO substrate. (b) Dependence of $(\alpha h\nu)^2$ of PMA and Cu: PMA films upon the incident photon energy ($h\nu$). (c) $J-V$ characteristics for the electron-only device with a structure of ITO/ZnMgO/QDs/ZnMgO:PVP/Al and the hole-only devices with a structure of ITO/PMA or Cu: PMA/TFB/BFTP/QDs/MoO₃/Al. (d) The band alignment diagram of PEDOT: PSS, Cu: PMA and TFB/BFTP layers.

Table S1 Summary of the device performance of QLEDs without treatment (pristine), with BFTP, with Cu:PMA & BFTP.

Sample	V _{on} (V)	Peak EQE (%)	Peak Lum (cd/m ²)
pristine	2.5	3.71	1792
PEDOT:PSS/TFB/BFT	1.8	8.13	14085
P			
Cu:PMA/TFB/BFTP	1.8	8.46	18356

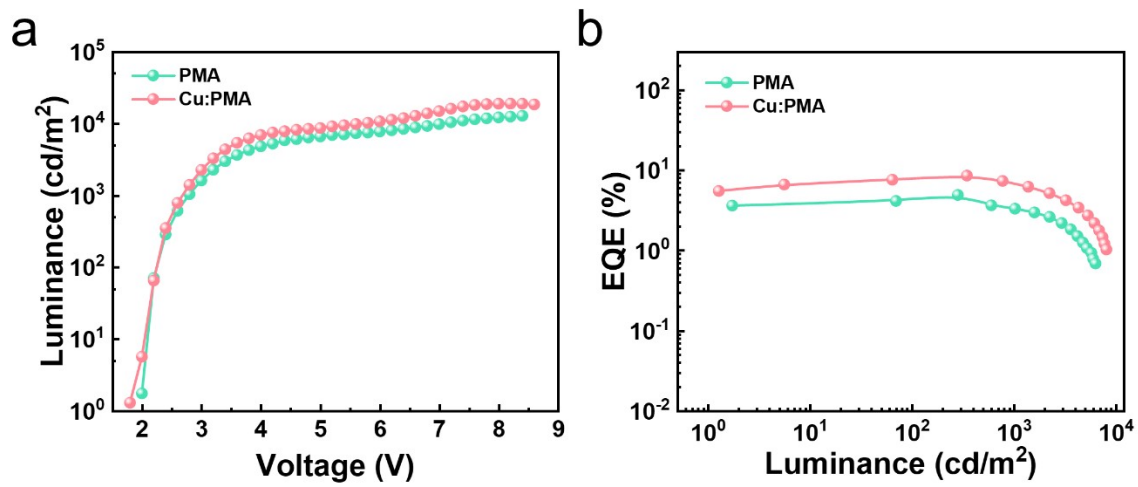


Figure S9 (a) L - V and (b) EQE - L characteristics of PEDOT:PSS-based and Cu:PMA-based QLEDs.

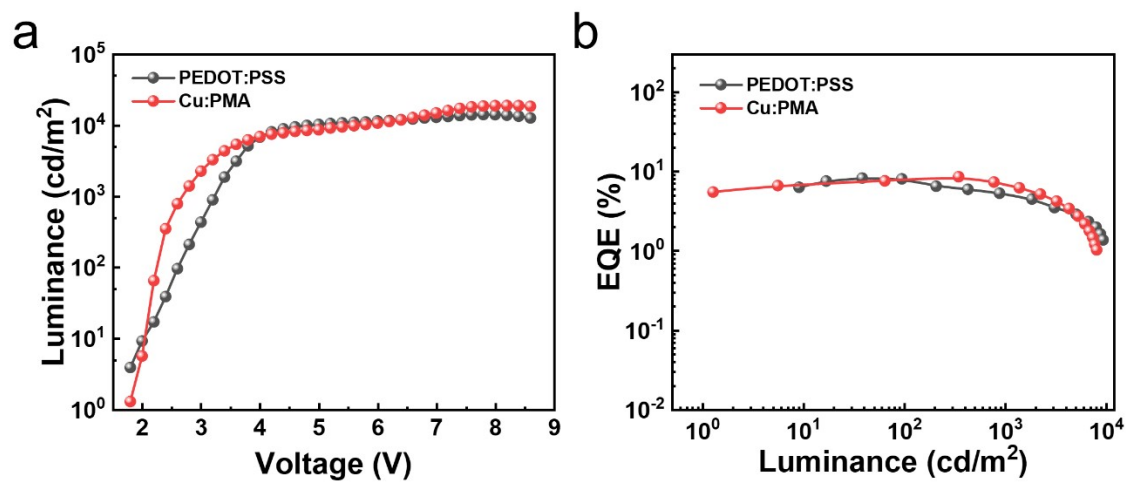


Figure S10 (a) L - V and (b) EQE - L characteristics of PEDOT:PSS-based and Cu:PMA-based QLEDs.

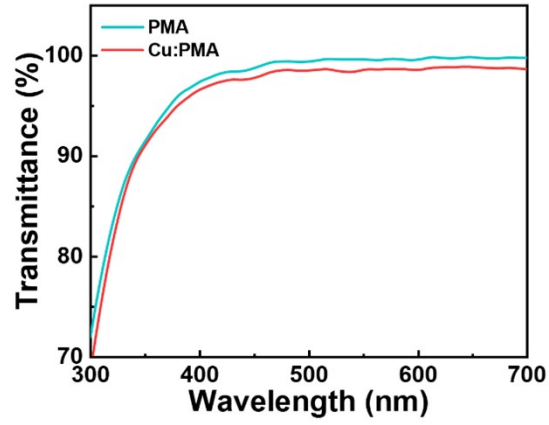


Figure S11 Transmittance spectra for the PMA and Cu: PMA films.

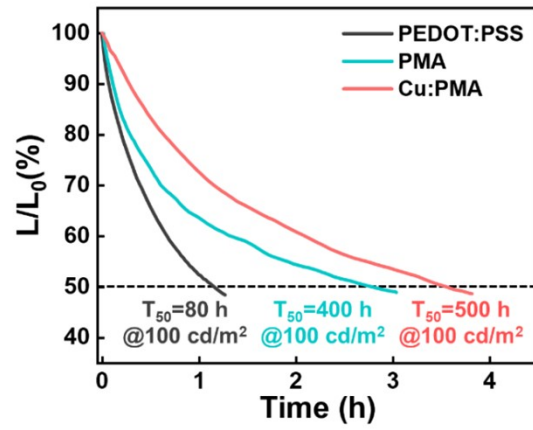


Figure S12 Operational lifetimes of BFTP-based QLEDs with different hole injection layers (PEDOT: PSS, PMA and Cu: PMA HILs).